ELSEVIER

Chemical Engineering Journal 84 (2001) 405–411

Chemical Engineering Journal

www.elsevier.com/locate/cej

Morphological structure of nanometer TiO_2–Al_2O_3 composite powders synthesized in high temperature gas phase reactor

Liyi Shi [a,*], Chunzhong Li [b], Aiping Chen [b], Yihua Zhu [b], Dingye Fang [b]

[a] *Department of Chemistry, Shanghai University, Shanghai 200072, PR China*
[b] *East China University of Science and Technology, Shanghai 200237, PR China*

Received 30 January 2000; received in revised form 9 August 2000; accepted 20 September 2000

Abstract

In this research, nanometer TiO_2–Al_2O_3 composite powders were synthesized by the gas-phase oxidation of $TiCl_4$ and $AlCl_3$ in a high temperature tubular aerosol flow reactor. The measurement of EDS, XPS, XRD and TEM were used to characterize the chemical composition, crystal structure, and size of the particles. The crystal structure of titania and alumina in composite particles was affected by the $AlCl_3$ and $TiCl_4$ feed ratio. Aluminum titanate was formed when residence time was 1.73 s, reaction temperature was 1400°C, and $AlCl_3$ and $TiCl_4$ feed ratio was 2.80. The effect of processing parameters on the particle size and distribution of composite particles was studied. As the preheating temperature of oxygen increased, average particle size of the composite particles became smaller and size distribution more uniform. Enhancement of flow rate of cooling gas injected into reactor tail was benefit controlling the particle size. The composite particle size increased, respectively, with increasing reaction temperature and residence time.

Keywords: Composite powder; Nanometer powder; Gas phase reaction

1. Introduction

To obtain high quality ceramic materials, the structure of the ceramic body must be controlled during fabrication. The structure, which develops during sintering, is largely determined by powder characteristics (e.g. particle size, size distribution, state of agglomeration, crystal structure, and chemical composition) [1,2]. The desirability for nanometer ceramic oxide powders with narrow size distribution has been reported by several authors [3,4]. TiO_2–Al_2O_3 composite ceramic has attracted considerable attention in view of its high strength and low thermal expansion coefficient [5,6]. It is very important to choose a suitable preparation route to obtain TiO_2–Al_2O_3 composite powders with small and uniform particle size. TiO_2–Al_2O_3 composite powders are usually prepared from a mixture of Al_2O_3 and TiO_2 powders, which are ground and mixed in a ball mill (or a mechanical mixer). Such method, however, often does not yield powders mixed homogeneously on a microscopic scale, and does not allow control of particle size and shape [7,8]. Wolgnier et al. [9] obtained TiO_2–Al_2O_3 composite powders by hydrolysis and polycondensation reaction of organometallic compounds of aluminum and titanium. This method has its drawbacks, the reagents used are expensive and the reaction time is very long. Okamura et al. [10] prepared TiO_2–Al_2O_3 composite powders by the hydrolysis of titanium alkoxide in an Al_2O_3 dispersion. To avoid serious agglomeration of the coated powder during hydrolysis, the solution of alkoxide and water need to be added stepwise to the Al_2O_3 dispersion. This process is hard to be scaled up for it is difficult to control the number of steps. Formation of particles in gas stream (aerosol processes) is routinely employed in manufacture of various commodities such as carbon blacks, pigmentary titania, fumed silica, zinc oxide, etc. The annual production of these materials amounts to several million tonnes worldwide [11–13]. Particle production in the gas phase processes is attractive because it provides rapid mixing on a molecular scale and energy. These processes offer advantages over the wet-chemistry processes. The product powder is usually readily separated from the gas, i.e. no post-processing such as calcination is needed, which is a common practice in wet processes. Furthermore, the effluent gases can be fairly easily cleaned for exhaust or recycling, in contrast to liquid byproducts. Because of the absence of a liquid dispersion medium (possibly containing surfactants), materials of high purity can be synthesized by aerosol conversion routes. Powder synthesis in the gas phase is carried out either by gas-to-particle conversion or by particle-to-particle conversion. With gas-to-particle

* Corresponding author. Tel.: +86-21-5633-1869.
E-mail address: qjfsly@online.sh.cn (L. Shi).

1385-8947/01/$ – see front matter
PII: S1385-8947(00)00282-5

Nomenclature

C_0	initial $TiCl_4$ concentration (mol/l)
Q	cooling gas rate (m^3/h)
t	residence time (s)
T	reaction temperature (°C)
T_{O_2}	oxygen preheating temperature (°C)
X_{inlet}	$AlCl_3/TiCl_4$ molar ratio in the reactant mixture

conversion, particles are built from molecules all the way up to the desired size. Several metal oxide powders such as titania, zinc oxide, and silica have been prepared by this process. To prepare pigmentary rutile titania, aluminum compounds have been used to adjust the morphological structure of titania in hot-wall or flame reactors [14–16]. Akhtar et al. [15] and Vemury et al. [16] revealed that the addition of $AlCl_3$ in high temperature gas-phase reactors results in predominantly the rutile form of ultrafine titania, but reduces the specific surface and increases the particle size of titania. Most of the previous studies have been centered on preparation of rutile titania, few works have been done for the aim of preparing nanometer TiO_2–Al_2O_3 composite particles. Also in these studies, little effort has been made to control the generated particles on nanometer scale. It has been suggested that multicomponent particles with controlled properties such as particle size, crystal structure, and morphology etc., which may be prepared by aerosol processes, be of great interest [17,18]. Hung et al. [19] synthesized TiO_2–Al_2O_3 composite powders using a counterflow diffusion flame burner. $Al(CH_3)_3$ and $TiCl_4$ were used as source materials for the formation of oxide particles in hydrogen–oxygen flames. In this research, little effort has been made to relate processing conditions to ultimate morphological structure of the as-produced TiO_2–Al_2O_3 composite powders.

In this paper, nanometer TiO_2–Al_2O_3 composite powders synthesized by $TiCl_4$ and $AlCl_3$ co-oxidation in a high temperature tubular aerosol flow reactor were characterized by EDS, XPS, XRD, TEM, and BET surface area analysis. The effect of process parameters such as oxygen preheating temperature, cooling gas rate, reaction temperature, and residence time on the particle size and distribution was investigated.

2. Experimental procedure

The raw materials used in this study were $TiCl_4$ (purity of 98%), $AlCl_3$ (purity of 98%), oxygen (purity of 99.99%), and NaOH (purity of 98%). The carrier gas was N_2 (purity of 99.99%).

A schematic of the experimental apparatus is shown in Fig. 1. The reaction apparatus consists of gas purification, reactant preheating, reaction, powder collection and off-gas treatment parts. The reactor was a 3.9 cm i.d. (4.8 cm o.d.), 95.0 cm long alumina tube that is externally heated in a horizontal furnace (Shanghai Sanya Furnace). The nitrogen gas, purified by a N_2 purifier, was divided into three parts. The first bubbled at 0.036 m^3/h through a $TiCl_4$ glass evaporator which was maintained at 80°C using a heated water bath. The $N_2/TiCl_4$ stream should passed through a preheater controlled at 435°C before it entered into the reactor. The second bubbled through a stainless steel $AlCl_3$ container whose temperature was adjusted from 130 to 160°C to change the $AlCl_3$ feed ratio. Its flow rate was at 0.07 m^3/h, except in the experiments for the determination of the effect of residence time. The $N_2/TiCl_4$ stream coming out of the preheater was mixed with $N_2/AlCl_3$ stream and then flowed into the reactor through the central tube of the reactor. The concentrations of $TiCl_4$ and $AlCl_3$ in the gas stream were determined by recording the weight of the halide containing vessels before and after each experiment. All lines transporting $TiCl_4$ and $AlCl_3$ were maintained at 150°C to prevent condensation of

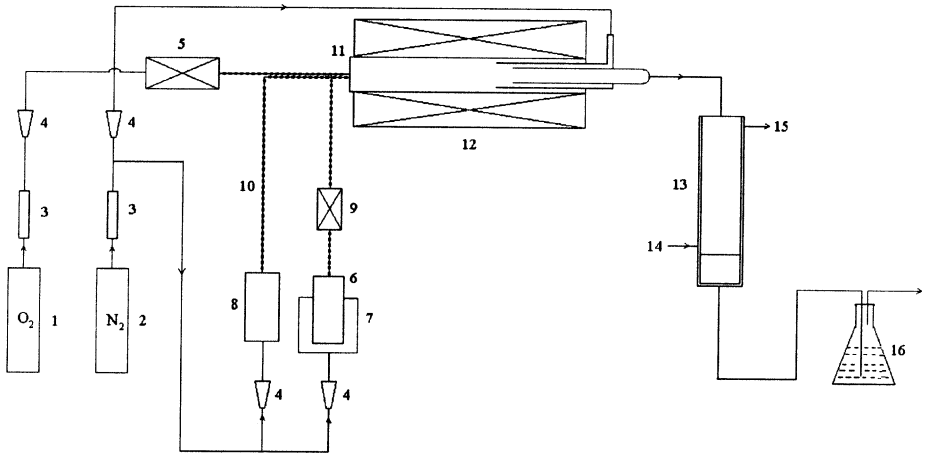

Fig. 1. Experimental apparatus for preparation of TiO_2 particles. (1) O_2 steel cylinder; (2) N_2 steel cylinder; (3) gas purifier; (4) flow indicator; (5) O_2 preheater; (6) $TiCl_4$ gasifier; (7) heated water bath; (8) $AlCl_3$ gasifier; (9) $TiCl_4$ preheater; (10) insulating lining; (11) reactor; (12) electric furnace; (13) particle collector; (14) cooling water inlet; (15) cooling water outlet; (16) chlorine absorber.

Table 1
Experimental condition list

Q (m^3/h)	X_{inlet} (mol/mol)	T_{O_2} (°C)	T (°C)	t (s)
0–0.036	0.09–1.14	600–870	1100–1500	1.36–1.73

$TiCl_4$ and $AlCl_3$ in the lines. The third, served as a cooling gas, was injected into the reactor tail at 0.036 m^3/h from the outer annulus, mixed with the reactor effluents, and the cooled gases exit the reactor through the inner tube. Oxygen gas, purified by an O_2 purifier, passed through a preheater at 0.08 m^3/h, and flowed into the reactor through the second tube of the reactor, and the flow of oxygen gas was usually in excess of the stoichiometric amount. The product was collected by using a Teflon membrane filter that has an average pore diameter of 200 nm. The reactor effluents were exhausted through the laboratory hood after scrubbing in a sodium hydroxide solution. All flows into the reactor were precisely controlled using mass flow controllers. The experimental conditions were listed in Table 1.

Elemental composition of the particles was determined by EDS (EDAX PV-9900, Hitachi) unit on scanning electron microscope (SEM, S-570, Philips). The surface chemical composition of particles was obtained by XPS (X-ray Photoelectron Spectroscopy, Perkin-Elmer PHI5000C ECSA System). XRD patterns of the powder samples were obtained using Rigaku DMAX/rB diffractometer and monochromated high intensity Cu $K\alpha_1$ radiation ($\lambda = 0.154$ nm). The diffraction pattern was taken with a scan rate of 4°/min over the range $5° < 2\theta < 80°$ at room temperature. Average grain sizes were calculated from the {1 1 0} rutile diffraction peak widths by using the Scherrer equation. TEM (JEM-1200EXII, Japan Jeol) was used to observe the morphology of the particles. TEM of these samples was done by ultrasonically dispersing the powders in water prior to deposition on a carbon-coated TEM grid. The particle size and size distribution were determined by counting more than 300 particles from TEM pictures. The geometric standard deviation of the particles was obtained from a log-probability plot.

3. Result and discussion

3.1. Chemical composition and crystal structure

EDS analysis shows that both titanium and aluminum are present in the particles. Fig. 2(a) shows a typical XPS scan of these powders. The scans show the presence of titanium, aluminum, oxygen, and carbon. Titanium has several oxidation states, but the deconvoluted Ti 2p spectrum (Fig. 2b) shows the presence of only Ti^{4+}. The binding energies of the Ti 2p3/2 and Ti 2p1/2 peaks (458.6 and 464.3 eV) are found to agree with the standard value (458.8 and 462.2eV in [17]). Hence, it is concluded that none of suboxides of titania are

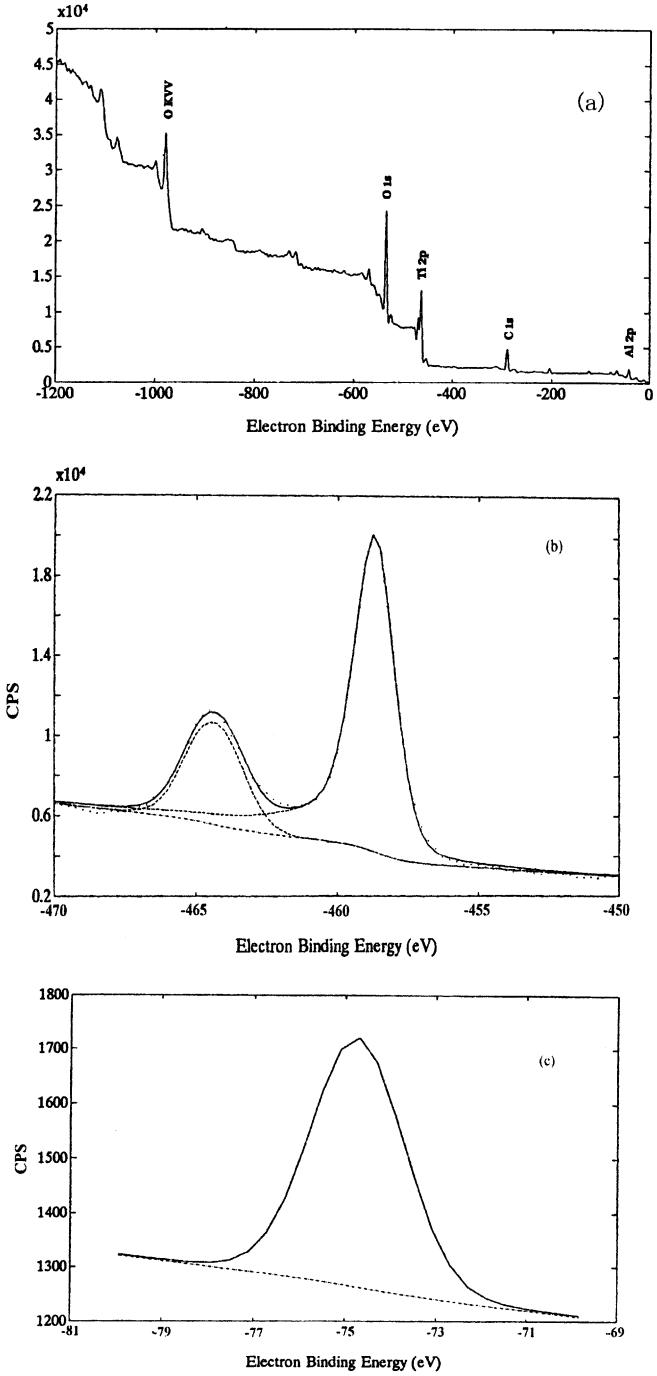

Fig. 2. XPS patterns of TiO_2–Al_2O_3 composite particles. (a) XPS scan of TiO_2–Al_2O_3 composite particles; (b) Ti 2p spectrum; (c) Al 2p spectrum.

formed. The Al 2p spectrum (Fig. 2c) shows that the Al 2p peak occurred at a binding energy of 74.5 eV which is close to the value of 74.4 expected for aluminum in aluminum oxide [20]. The carbon peak is attributed to the organic materials used to hold the powders in the vacuum chamber of the instrument. Fig. 3 shows that the XRD patterns for the TiO_2–Al_2O_3 powders synthesized at different $AlCl_3/TiCl_4$ feed ratios when $T = 1400$°C, $t = 1.73$ s, $T_{O_2} = 870$°C,

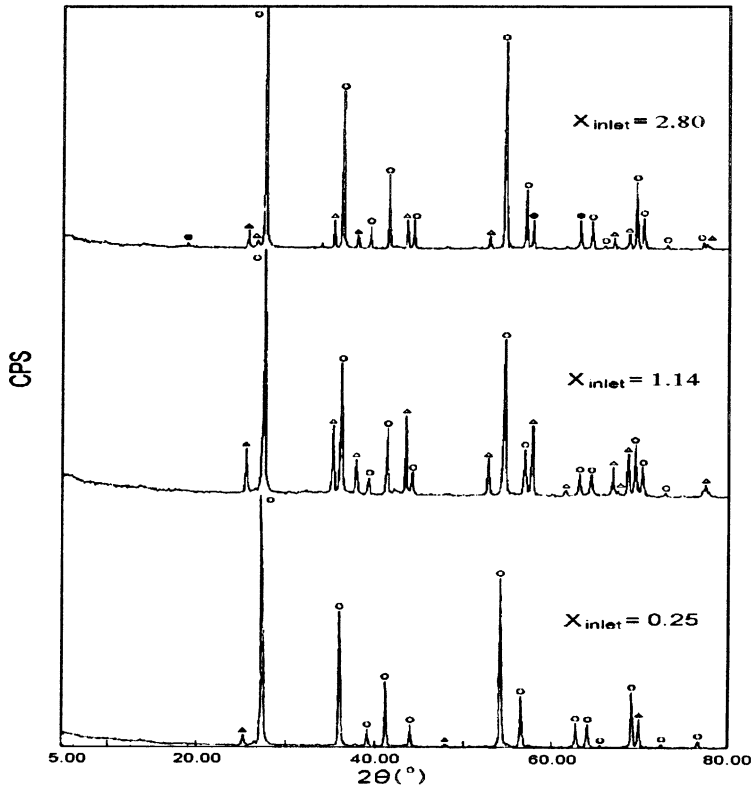

Fig. 3. XRD patterns of TiO_2–Al_2O_3 composite particles. (●) Al_2TiO_5; (▲) anatase TiO_2; (○) rutile TiO_2; (△) α-Al_2O_3.

and $Q = 0.036\,m^3/h$, both anatase TiO_2 diffraction peaks ($2\theta = 25.3°$) and rutile TiO_2 diffraction peaks ($2\theta = 27.5°$) exist. By comparing the relative intensities of the strongest peaks corresponding to anatase and rutile, one can see that the main phase of TiO_2 is rutile. Though $AlCl_3$ is routinely used as a rutile promoter in TiO_2 pigment manufacture, exist of small amount of anatase in this experiment is related to the anatase to rutile transformation mechanism in aerosol reactors. It has been suggested that TiO_2 phase composition prepared by $TiCl_4$ gas-phase high temperature oxidation is affected by reactor style, process parameters such as mixing conditions of reactants, reaction temperature, $AlCl_3$ concentration, residence time, etc. [21,22]. In earlier studies the authors revealed the addition of $AlCl_3$ can enhance the rutile weight fraction, but the effect of reaction temperature was more important. A maximum rutile fraction was attained at 1200°C and $AlCl_3$ and $TiCl_4$ feed ratio of 0.09. The existence of the maximum mass fraction of rutile can be explained by the anatase to rutile transformation mechanism in hot-wall reactor [21,22]. When $X_{inlet} = 0.25$, There is little evidence from the XRD pattern on the existence of any third phase like Al_2O_3. Because XPS measurement shows that aluminum oxide is present in the powders, mostly amorphous aluminia is formed which is not detected by XRD. When $X_{inlet} = 1.14$, there exist the α-Al_2O_3 diffraction peaks ($2\theta = 43.3, 66.5, 68.2°$) besides the anatase and rutile TiO_2 diffraction peaks. The result indicates that both TiO_2 and α-Al_2O_3 are present in the composite particles. When $X_{inlet} = 2.8$, the powders are composed of TiO_2, α-Al_2O_3, and Al_2TiO_5. Because aluminum titanate Al_2TiO_5 diffraction peaks ($2\theta = 26.6$, 33.9, 37.9, 51.8, and 57.9°) are observed besides TiO_2 and α-Al_2O_3 diffraction peaks.

3.2. Morphology and particle size

Fig. 4 shows TEM pictures of composite powders produced at different preheating temperature of oxygen when $T = 1300°C$, $X_{inlet} = 0.09$, $t = 1.73\,s$, and $Q = 0.036\,m^3/h$. The average particle size of the powders was 118, 89 and 36 nm, the geometric standard deviation, which represents the size distribution, was 1.53, 1.48 and 1.41, respectively, when $T_{O_2} = 600$, 700 and 870°C. This means that average particle size of composite powders becomes smaller and size distribution more uniform as the preheating temperature of oxygen increases. In gas-to-particles conversion, nanometer particles are formed through chemical reaction, nucleation, growth, and coagulation and sintering of grains, in which nucleation is a key step [12]. The nucleation rate can be given as [23]

$$I = I_0 \sigma^{1/2} \left(\frac{p}{T}\right) \exp\left(\frac{-16\pi\sigma^3 M^2}{3P^2R^2T^2 \ln^2 SR}\right) \quad (1)$$

where T is temperature, P is pressure, M is molecular weight, σ is surface tension, SR is saturation degree. Although the

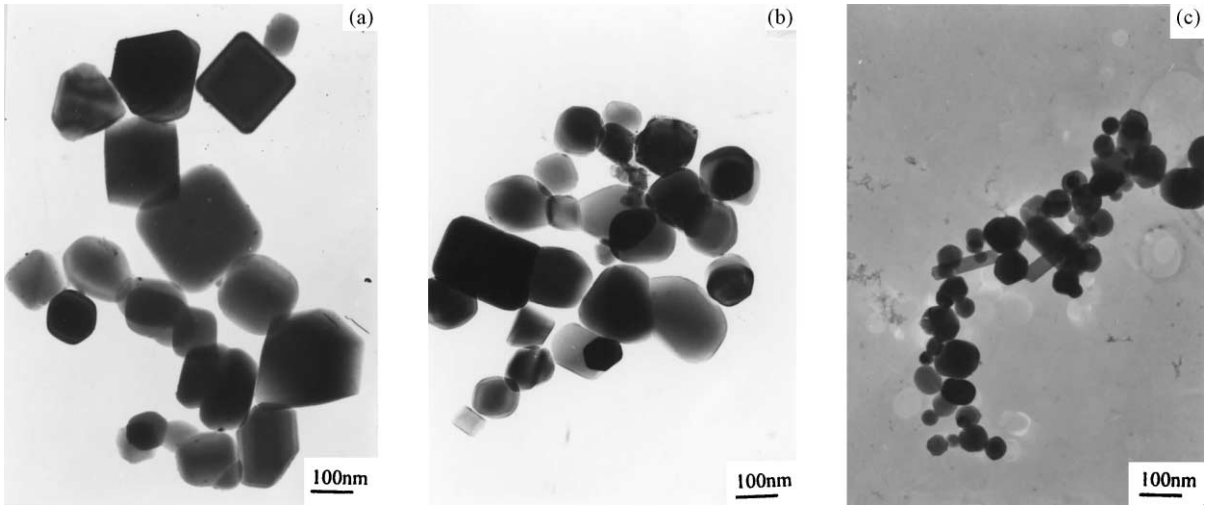

Fig. 4. TEM photograph of TiO_2–Al_2O_3 composite particles synthesized at different T_{O_2}. (a) $T_{O_2} = 600°C$; (b) $T_{O_2} = 700°C$; (c) $T_{O_2} = 870°C$.

important factors influencing nucleation rate are temperature, saturation degree and product surface tension, the saturation degree is prominent (Eq. (1)). Nanometer powders can be prepared in the gas phase reactor only at high product saturation degree. As the preheating temperature of oxygen increases to the reaction temperature, the reactants will meet each other at the exact reaction temperature. Then the nucleation particles may be developed since a high saturation degree of the product leads to a high nucleation rate at high preheating temperature of oxygen. Therefore the number of nuclei increases with increasing of preheating temperature of oxygen. Because the average particle size is inversely proponent to the nucleus numbers [24], particles produced at such preheating conditions have smaller particle size and more uniform size distribution. When the preheating temperature of oxygen is lower than the reaction temperature, nucleation progressed from lower temperature to the reaction temperature heterogeneously. Thus, nuclei produced at low temperature have enough time to grow and serve as seeds. As a result, powders produced at low temperatures have a larger particle size and wider size distribution than powder produced at the higher preheating temperature. The authors [21] and Jang et al. [25] had studied the effect of preheating temperature of reactants on pure TiO_2 particle morphology. The synthesis of TiO_2–Al_2O_3 composite particles also revealed the similar trend, i.e. the preheating of reactants is an important factor in controlling the nucleation and consequently particle sizes and size distribution in high temperature gas-to-particle convention.

Fig. 5 shows TEM pictures of TiO_2–Al_2O_3 powders produced at different rate of cooling gas when $T_{O_2} = 870°C$, $X_{inlet} = 0.25$, $T = 1400°C$, and $t = 1.73$ s. When there was no cooling gas injected into reactor tail, aggregates of bigger particles are formed. The particles become smaller and

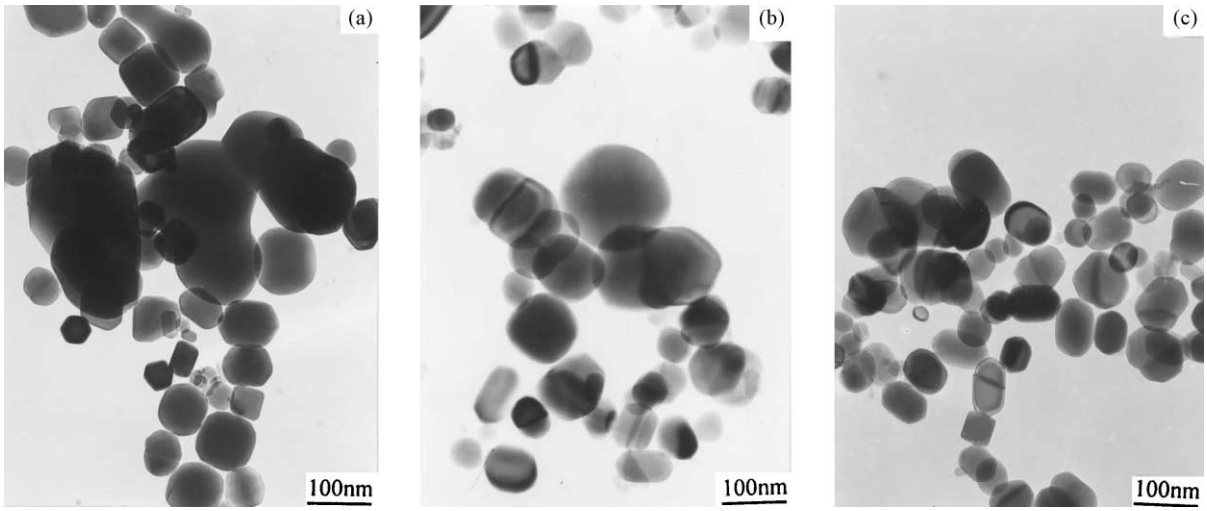

Fig. 5. TEM photograph of TiO_2–Al_2O_3 composite particles synthesized at different Q. (a) $Q = 0$; (b) $Q = 0.012\,m^3/h$; (c) $Q = 0.036\,m^3/h$.

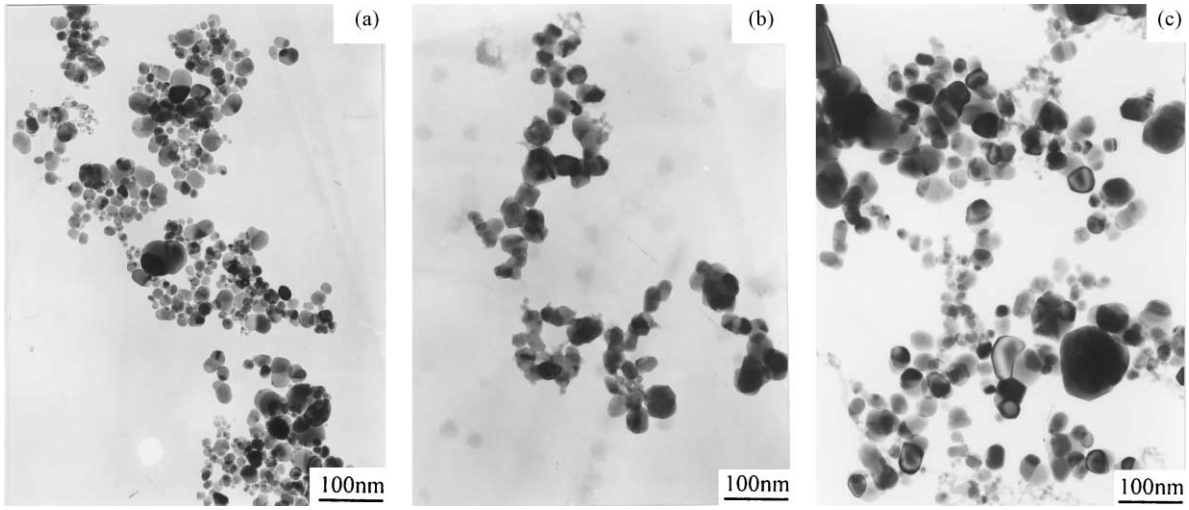

Fig. 6. TEM photograph of TiO_2–Al_2O_3 composite particles synthesized at different reaction temperatures. (a) $T = 1100^\circ C$; (b) $T = 1200^\circ C$; (c) $T = 1500^\circ C$.

size distribution more uniform with increasing of the rate of the cooling gas. In gas-to-particles conversion, the precursor vapor and gas react to form particles that grow further by surface reaction, coagulation, and sintering as they experience lower temperature downstream in the reactor, often resulting in agglomerate or aggregate of primary particles [17]. When the cooling gas is injected into the reactor tail, it immediately mixed with the reactor effluents, quenches surface reaction and inhibits particle growth by coagulation and sintering outside the reaction zone. Thus powders produced at higher cooling gas rate have a smaller particle size and narrower size distribution than those produced at lower cooling gas rate or those produced under no cooling gas.

When $X_{\text{inlet}} = 1.14$, $t = 1.73\,\text{s}$, $Q = 0.036\,\text{m}^3/\text{h}$, and $T_{O_2} = 870^\circ C$, the average grain size of the powders calculated from the line broadening by XRD using Scherrer's equation is 18.9, 31.4 and 57.8 nm, respectively, when $T =$ 1100, 1200 and 1500°C. Fig. 6 shows TEM pictures of these composite powders, and the average particle size is 24, 39 and 65 nm, respectively. This is in reasonable agreement with the measurement from the XRD. It can be seen from the measurement of XRD and TEM that increasing the reaction temperature led to an increase in particle size. During the fine particle formation process in gas phase reactor, many phenomena occur simultaneously, such as particle generation, particle growth and agglomerate formation, and morphology changes of the generated particles. Coagulation and sintering are especially important for controlling the particle size and structure in gas phase processes [13]. At higher temperature, a higher concentration of precursor monomers is obtained through a faster reaction rate that increases the collision frequency and leads to an increase in the size of the generated particles. Furthermore, there is an increase in grain boundary diffusion in TiO_2 and Al_2O_3 as the reaction temperature increases leading to faster sintering and larger particle size.

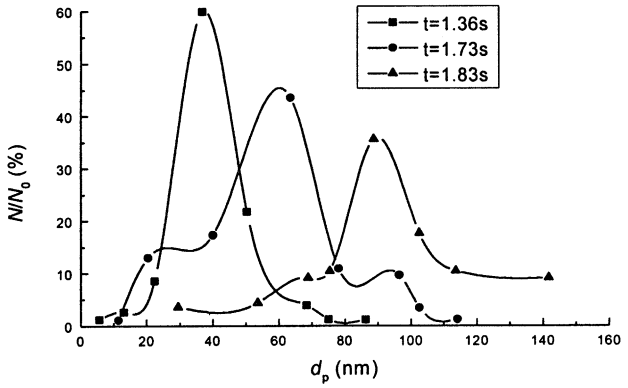

Fig. 7. The effect of residence time on average TiO_2–Al_2O_3 composite particle size.

Fig. 7 shows the effect of residence time in the reaction zone on the particle size and distribution when $T = 1400^\circ C$, $X_{\text{inlet}} = 0.09$, $T_{O_2} = 870^\circ C$, and $Q = 0.036\,\text{m}^3/\text{h}$. The average particle size was 38, 56 and 85 nm, and the geometric standard deviation was 1.41, 1.48 and 1.49, respectively, when $t = 1.36$, 1.73 and 1.83. In gas phase reactor, the initial stage of particle formation is nucleation, but at the later stage, the nucleation ceased, while the particles continue to grow. If residence time prolonged, the particles produced have more time for surface reaction, coagulation, and sintering. This leads to larger particle size and less uniform distribution.

4. Conclusion

Nanosized TiO_2–Al_2O_3 composite powders were synthesized by the gas-phase oxidation of $TiCl_4$ and $AlCl_3$ in a high temperature tubular aerosol flow reactor. The crystal structure of titania and alumina in composite particles

was affected by the $AlCl_3$ and $TiCl_4$ feed ratio. Aluminum titanate was formed when residence time was 1.73 s, reaction temperature was 1400°C, and $AlCl_3$ and $TiCl_4$ feed ratio was 2.80. As the preheating temperature of oxygen increased, average particle size of the composite particles became smaller and size distribution more uniform. Enhancement of flow rate of cooling gas injected into reactor tail was benefit controlling the particle size. The composite particle size increased, respectively, with increasing reaction temperature and residence time.

Acknowledgements

This research was supported by National Natural Science Foundation of China (No. 29636010) and The Ninth Five-year Project of National Planning Committee (No. 96-554-02).

References

[1] H.K. Bowen, Basic research needs on high temperature ceramics for energy applications, Mater. Sci. Eng. 44 (1980) 1.
[2] B. Fegley, E.A. Barringer, H.K. Bowen, Synthesis and characterization of monosized doped TiO_2 powders, J. Am. Ceram. Soc. 67 (1) (1984) C113.
[3] F.F. Lange, Powder processing science and technology for increased reliability, J. Am. Ceram. Soc. 72 (1989) 3.
[4] G. Yang, H. Zhuang, P. Biswas, Characterization and sinterability of nanophase titania particles processed in flame reactors, Nanostructured Mater. 7 (1996) 675.
[5] H.A.J. Thomas, R. Stevens, Aluminum titanate-a literature review part. 1. Microcracking phenomena, Br. Ceram. Trans. J. 88 (4) (1989) 144.
[6] H.A.J. Thomas, R. Stevens, Aluminum titanate — a literature review. Part 2. Engineering properties and thermal stability, Br. Ceram. Trans. J. 88 (5) (1989) 184.
[7] B. Freudenberg, A. Mocellin, Aluminum titanate formation by solid-state reaction of fine Al_2O_3 and TiO_2 powders, J. Am. Ceram. Soc. 70 (1987) 33.
[8] B. Freudenberg, A. Mocellin, Aluminum titanate formation by coarse Al_2O_3 and TiO_2 powders, J. Am. Ceram. Soc. 71 (1988) 22.
[9] T. Woignier, P. Lespade, J. Phalippou, R. Rogier, Al_2O_3–TiO_2 and Al_2TiO_5 ceramic materials by the sol–gel process, J. Non-Crystalline Solids 100 (1988) 325.
[10] H. Okumura, E.A. Barringer, H.K. Bowen, Preparation and sintering of narrow-sized Al_2O_3–TiO_2 composite powders, J. Am. Ceram. Soc. 69 (2) (1986) C22.
[11] L.Y. Shi, C.Z. Li, D.Y. Fang, J.P. Zhang, Y.H. Zhu, A.P. Chen, Ultrafine titania photocatalytic materials synthesized by high temperature reaction in $TiCl_4$–O_2 system, J. Inorg. Mater. 14 (1999) 717 (in Chinese).
[12] K.A. Kusters, S.E. Pratsinis, Strategies for control of ceramic powder synthesis by gas-to-particle conversion, Powder Technol. 82 (1995) 79.
[13] P. Stamatakis, C.A. Natalie, B.R. Palmer, W.A. Yuill, Research needs in aerosol processing, Aerosol Sci. Technol. 14 (1991) 316.
[14] Y. Suyama, A. Kato, Effect of additives of the formation of TiO_2 particles by vapor phase reaction, J. Am. Ceram. Soc. 68 (1985) C154.
[15] M.K. Akhtar, S.E. Pratsinis, Vapor phase synthesis of Al-doped titania powders, J. Mater. Res. 9 (5) (1994) 1241.
[16] S. Vemury, S.E. Pratsinis, Dopants in flame synthesis of titania, J. Am. Ceram. Soc.78 (1995) 2984.
[17] F.E. Kruis, H. Fissan, A. Peled, Synthesis of nanoparticles in the gas phase for electronic, optical and magnetic applications-a review, J. Aerosol Sci. 29 (5/6) (1998) 511.
[18] S.E. Pratsinis, S. Vemury, Particle formation in gases: a review, Powder Technol. 88 (1996) 267.
[19] C.-H. Hung, E.P. Miquet, J.L. Katz, Formation of mixed oxide powders in flames. Part II. SiO_2–GeO_2 and Al_2O_3–TiO_2, J. Mater. Res. 7 (7) (1992) 1870.
[20] S.H. Liu, D.G. Wang, C.Q. Pan, X-ray Photoelectron Spectroscopy Analysis, Science Press, Beijing, Vol. 305, 1988, p. 313 (in Chinese).
[21] L.Y. Shi, C.H. Li, A.P. Chen, Y.H. Zhu, D.Z. Cong, D.Y. Fang, Morphology and structure of nanosized TiO_2 particles synthesized in high temperature aerosol reactor, J. ECUST 25 (2) (1999) 151 (in Chinese).
[22] L.Y. Shi, C.Z. Li, D.Y. Fang, Research advance in vapor-phase synthesis of ultrafine titania particles, Mater. Rev. 12 (1998) 23 (in Chinese).
[23] C.Z. Li, B. Hua, Preparation of nanocrystalline SnO_2 thin film coated Al_2O_3 ultrafine particles by fluidized chemical vapor chemical deposition, Thin Solid Films 310 (1997) 238.
[24] J.G. Yu, Application of vapor-phase reaction in ultrafine powder synthesis, Chem. Bull. 10 (1991) 25 (in Chinese).
[25] H.D. Jang, J. Jeong, The effect of temperature on particle size in the gas-phase production of TiO_2, Aerosol Sci. Technol. 25 (1995) 553.